PHYSICAL REVIEW B **71**, 020103(R) (2005)

Stress and orientation in the relaxor/ferroelectric superlattices $(PbMg_{1/3}Nb_{2/3}O_3)_{(1-x)\Lambda}/(PbTiO_3)_{x\Lambda}$

H. Bouyanfif, M. El Marssi,* N. Lemée, F. Le Marrec, and M. G. Karkut
Laboratoire de Physique de la Matière Condensée, Université de Picardie Jules Verne, 33 rue Saint-Leu 80039 Amiens Cedex, France

B. Dkhil
Laboratoire Structure Propriétés et Modélisation des Solides, UMR 8580, Ecole Centrale Paris, Grande Voie des Vignes, 92295 Châtenay-Malabry Cedex, France

(Received 6 August 2004; published 31 January 2005)

We have grown a series of $[PbMg_{1/3}Nb_{2/3}O_3]_{(1-x)\Lambda}/[PbTiO_3]_{x\Lambda}(PMN_{1-x}/PT_x)$ superlattices for which the composition varies, $0.1 \leqslant x \leqslant 0.8$, but the modulation period Λ is kept constant at about 130 Å. X-ray diffraction indicates that the polar *c* axis of the PT layers lies in the plane of the films. The Raman spectra, which reflect the sum of the spectra of PMN and the PT layers, confirm the *a*-domain orientation of the PT layers. A downshift of the $E(1TO)$ soft mode of the PT layers was attributed to tensile stress, estimated to be in the range of 2.5–3.6 GPa, induced by the lattice mismatch of PMN/PT layers. We observe the splitting of the "silent" mode in PT into distinct modes B_1 and E and attribute this to the strains present in the layers.

DOI: 10.1103/PhysRevB.71.020103 PACS number(s): 68.65.Cd, 77.84.−s, 78.30.−j

The relaxor ferroelectric $PbMg_{1/3}Nb_{2/3}O_3$ (PMN) can be combined with the ferroelectric $PbTiO_3$ (PT) to form a solid-solution $Pb[(Mg_{1/3}Nb_{2/3})_{1-x}Ti_x]O_3$ (PMN_{1-x}-PT_x), which can have either relaxor or ferroelectric properties depending on x.[1,2] Nominally cubic at all temperatures, relaxors are in fact structurally inhomogeneous materials in which polar nanosized regions are randomly distributed in a nonpolar matrix.[3] PMN ($a_{PMN}=4.048$ Å) exhibits characteristic relaxor behavior characterized by a strong frequency dependence of the peak in the permittivity as a function of temperature.[4] In contrast, bulk PT undergoes a structural phase transition at 763 K and is highly tetragonal ($c_{PT}=4.15$ Å and $a_{PT}=3.898$ Å). The PMN_{1-x}-PT_x solid solution evolves from a relaxor to a normal ferroelectric and near the morphotropic phase boundary ($x \sim 0.35$), extremely large electromechanical coupling constants have been measured on single crystals.[1,2] Thus this material is a promising candidate for actuator and transducer applications not only in bulk but also in thin film form.

Evidence for typical relaxor behavior in PMN films has been reported by several groups.[5–10] Nevertheless, compared to single crystals, differences in the physical properties, such as lower permittivity and electromechanical coupling coefficients, have been reported.[5–9] The influence of the misfit between film and substrate, interfacial layers, and microstructural defects are invoked to explain the measured electrical and electromechanical properties of thin films.

PT films have been extensively studied experimentally and theoretically. Depending on the misfit between PT and the substrate, different domain states can be expected in the ferroelectric phase. Theoretical works[11–13] predict three domain configurations: single *c* axis, single *a* axis, and twin domain *c*/*a*/*c*/*a*-type states. To date, only *c* axis and *c*/*a*/*c*/*a* polydomains have been reported experimentally for PT films.[14–16] However, when PT is a superlattice (SL) constituent such as in $PbTiO_3/BaTiO_3$ (PT/BT) SL's,[17] we have conclusively shown by x-ray diffraction (XRD) and Raman spectroscopy that the PT layers have their polar axis oriented in the plane of the film.

Here we report the fabrication and structural characteristics of SL's of alternating layers of PMN and PT. Our long-term aim is to study the interactions between a relaxor and a ferroelectric, to investigate the effects of size and strain on relaxor and ferroelectric layers, and to compare the physical properties of PMN/PT SL's with their solid-solution counterparts. We have grown six different SL's of the type $[PMN_{(1-x)\Lambda}/PT_{x\Lambda}]_{10}$, where $x=0.1$, 0.2, 0.35, 0.4, 0.5, 0.8, Λ is approximately 130 Å, and the total number of periods for each SL is 10. We chose the ratios of PMN to PT to correspond to different regions of the PMN-PT solid-solution phase diagram. This choice was motivated by the eventuality of constructing PMN/PT SL's in the zero wavelength limit, thus producing a SL more closely resembling a solid-solution material. In this way we might artificially construct an epitaxial solid solution whose properties we could compare to those of bulk PMN-PT solutions. We present XRD and Raman results on these SL's grown on single crystal MgO ($a_{MgO}=4.213$ Å) buffered with the conducting oxide $La_{1/2}Sr_{1/2}CoO_3$ (LSCO, $a_{LSCO}=3.805$ Å). MgO was chosen as a substrate because its Raman modes are inactive thus allowing us better access to the film spectra.

The samples were grown by pulsed laser deposition using a Spectra Physik 248-nm laser in a MECA 2000 UHV chamber. A 1500 Å LSCO buffer/electrode layer was deposited at a substrate temperature (T_s) of 700 °C and 0.2 mbar oxygen partial pressure (P_{O2}). The temperature and oxygen pressure for PMN and PT layers were, respectively, $T_s=545$ °C and $P_{O2}=0.3$ mbar, and $T_s=600$ °C and $P_{O2}=0.3$ mbar. The deposition rate (0.2 Å/pulse) was determined from the x-ray thickness oscillations observed on films of PMN and of PT. The deposition system is equipped with a 15-kV reflection high-energy electron diffraction (RHEED) system, which enables us to monitor the surface quality of the layers. The RHEED streaks we observe from the PMN and PT layers indicate cube-on-cube epitaxial growth.

Standard $\theta-2\theta$ x-ray diffractometry was performed on all samples using a two-circle Siemens D5000 diffractometer

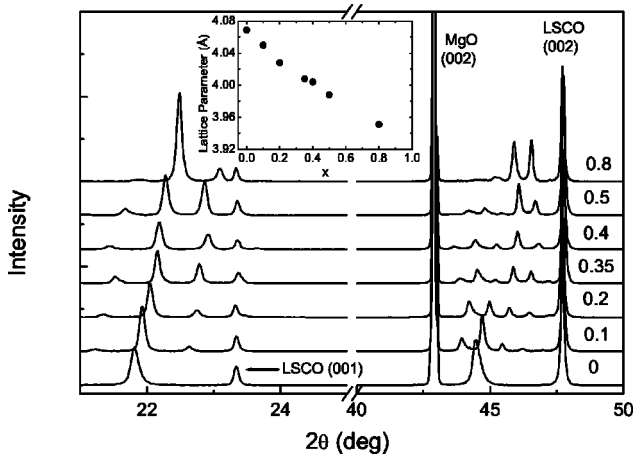

FIG. 1. θ–2θ x-ray diffraction for $PMN_{(1-x)\Lambda}/PT_{x\Lambda}$ SL's for $0.1 \leqslant x \leqslant 0.8$ and for an $x=0$, 1500-Å-thick PMN film. The inset shows the x dependence of the SL average lattice parameter.

with Cu $K\alpha$ radiation. Figure 1 shows seven diffractograms taken on PMN_{1-x}/PT_x for $0 \leqslant x \leqslant 0.8$. No pyrochlore phase is present within the detection limits of our instruments. The presence of satellite peaks implies chemically modulated structures and the angular distance between the peaks determines Λ. The evolution of the peaks positions and intensities reflect the change in the composition of the SL's from the PMN-rich wavelengths to the PT-rich wavelengths. This is also conveyed in the inset which is a plot of the average SL lattice parameter a_{SL} as a function of the PT concentration x. a_{SL} is a weighted average of the modulation wavelength $\Lambda = N_1 d_1 + N_2 d_2$, where N_1 and N_2 are the number of unit cells in the modulation period and d_1 and d_2 are the lattice parameters of the constituents. Using $n\lambda_x = 2\Lambda \sin \Theta_n$ to calculate the average lattice parameter $a_{SL} = \Lambda/n$ of the SL, where we select Θ_n to be the most intense satellite peak. The out-of-plane a_{SL} decreases linearly from a value close to that of PMN when the proportion of PT is small, and extrapolates, at $x=1$, to a value of 3.92 Å, which is close to the a-axis parameter of PT. Preliminary model calculations, following those of Ref. 17 of the experimental positions and amplitudes also support a structure in which the a axis of the PT layers in PMN/PT SL's is perpendicular to the plane of the film. We have previously reported the a-axis PT layer orientation of PT/BT SL's.[17] Since the bulk parameters of BT ($c=4.03$ Å, $a=3.99$ Å) are slightly smaller than of PMN, our results, combined with those reported by Jiang *et al.*[18] on c-axis PT layers in closely matched $PbTiO_3/SrTiO_3$ SL's, is consistent with the idea that the orientation of PT layers is strongly dependent on the relative mismatch of the SL constituents. However there has yet to be a theoretical treatment of SL systems that puts this orientational dependence on a quantitative basis as has been done for films in Refs. 11–13.

Raman measurements were performed in a backscattering geometry using the 514.5-nm-line from an argon ion laser focused to a spot of 1 μm in diameter. The scattered light was analyzed using a Jobin Yvon T64000 spectrometer and collected with a charge-coupled device. Polarized spectra have been recorded with respect to the crystallographic axes of a-domain PT layers: Y is perpendicular to the MgO substrate, $X//[100]_{MgO}$, and $Z//[010]_{MgO}$. Studies on PT single crystals have shown that selection rules are strictly respected for both the ferroelectric and paraelectric phases. By monitoring the $E(1TO)$ soft mode, which is very sensitive to the pressure in PT bulk,[19,20] it is possible to estimate the stress in PT films[21–23] and in PT layers in PT-based SL's.[17]

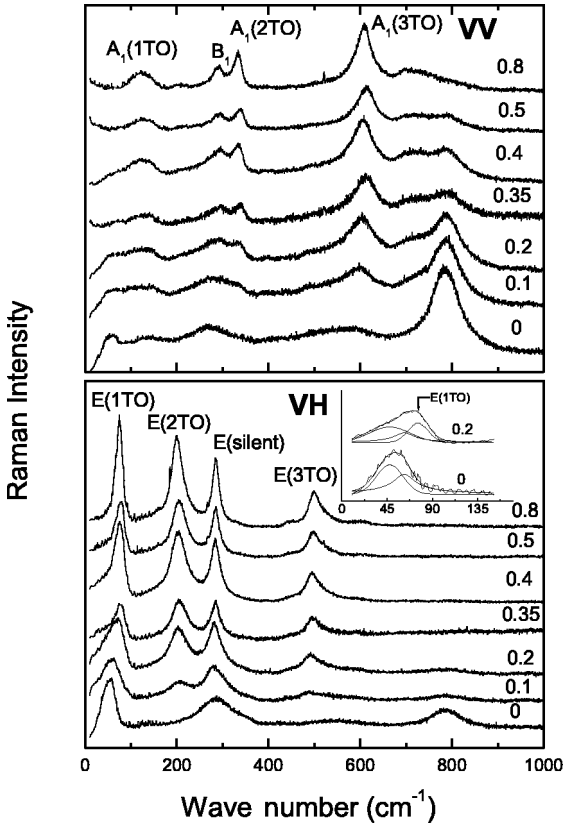

FIG. 2. Room-temperature Raman spectra VV and VH for $PMN_{(1-x)\Lambda}/PT_{x\Lambda}$ SL's $0.1 \leqslant x \leqslant 0.8$ and for an $x=0$, 1500-Å-thick PMN film. The labeling corresponds to the PT modes (see Table I). The inset shows examples of the fits for the low-frequency band using three peaks, two of which correspond to PMN modes ($x=0$) and the third to the $E(1TO)$ mode of PT for $x=0.2$.

Figure 2 shows room-temperature Raman spectra recorded in $Y(XX)\bar{Y}(VV)$ and $Y(XZ)\bar{Y}(VH)$ scattering geometries for the PMN_{1-x}/PT_x SL's and for an $x=0$, 1500-Å-thick PMN film. The polarization-dependent spectra of the $x=0$ PMN film confirm its epitaxial quality. Unlike PT films and SL's, the Raman line frequencies and profiles of the $x=0$ film are essentially the same as those measured for PMN single crystals.[24] This is interesting since we have reported a tetragonal distortion c/a in PMN films that increases with the decreasing film thickness.[10] In spite of this distortion, both the Raman and electrical measurements[9] show that the films remain relaxors. As with PMN single crystals, the ratio I_{VH}/I_{VV} of the 785-cm^{-1}-mode is much less than unity. This can be interpreted as a signature of relaxor PMN: the ratio $I_{VH}/I_{VV}=1$ signals the onset of the rhombohedral ferroelectric order in PMN-PT crystals.[25] Since the mode frequencies of the PMN films are the same as those of single crystals, we can conclude that the Raman spectra are insensitive to biaxially strained PMN films. Also in Fig. 2, the 785-cm^{-1} VV

TABLE I. Frequencies (in cm^{-1}) of the observed Raman modes in a $PbTiO_3$ single crystal and the $x=0.8$ PMN/PT SL.

Mode labeling[a]	Single crystal PT[a]	superlattice
$E(1TO)$	87.5	76
$A_1(1TO)$	148.5	123
$E(2TO)$	218.5	200
B_1+E	289	287(E)
		296(B_1)
$A_1(2TO)$	359.5	333
$E(3TO)$	505	500
$A_1(3TO)$	647	608

[a]For PT single crystal. Reference 28.

line for the SL's occurs at the same frequency as for the $x=0$ PMN film. This suggests that the Raman lines of the PMN layers in the SL are also not affected by the strain. We are of course aware of the work by Kreisel *et al.*[26] on bulk single-crystal PMN that shows that the Raman spectrum is sensitive to hydrostatic pressure. They have reported a frequency variation of certain modes with pressure including the mode at $\sim 785\ cm^{-1}$. This is an interesting result and the differences between spectra of the strained layers of PMN in film and SL's and that of PMN bulk under hydrostatic pressure could provide additional clues as to the microscopic origin of relaxors.

The spectral profile for the SL rich in PT of Fig. 2 is comparable to that of PT single crystal. As x decreases, we observe spectra that reflect the sum of the spectra of PT and PMN. This is clearly apparent in *VV* spectra where the $785\ cm^{-1}$ mode, the most intense peak of the PMN film, is observed in all SL's except for $x=0.8$. Since the Raman signal from PT is more intense than that from PMN, the PT peaks are clearly visible even for small x. The weak PMN signal in the $x=0.8$ SL is also the result of a small scattering volume.

Since the point group symmetry of the tetragonal ferroelectric phase of PT bulk is C_{4v}, cross polarization (xz and yz) will detect only E modes, parallel polarization (xx) and (yy) will detect both A_1 and B_1 phonons, while the (zz) polarization is needed to isolate the A_1 modes. For the $x=0.8$ PT-rich SL, there is a one-to-one correspondence between the Raman peaks and those of PT single crystals.[27,28] A_1 and B_1 modes are observed in *VV* geometry and E modes in *VH* geometry, which prove that the c-polar axis of the PT layers is parallel to the film and thus confirms the x-ray results. Table I gives the mode assignments and frequencies for the $x=0.8$ SL, and a PT single crystal. We note a significant downshift for the SL modes compared with those for the bulk, especially the $E(1TO)$, $A_1(1TO)$, $A_1(2TO)$ and $A_1(3TO)$ modes that are most sensitive to pressure.[19,20] We attribute the downshift, also observed in PT films[21–23] and in the PT layers of Ref. 17, to internal stresses induced by the mismatch between PMN and PT layers.

We estimate the stress in the PT layers by following the dependence of the $E(1TO)$ soft mode as a function of x. Since the PMN and PT layers contribute to the Raman spectra of PMN/PT SL we fit the low-frequency band of the *VH* spectra with the sum of three peaks: two PMN modes at 47 and $62\ cm^{-1}$, and one PT $E(1TO)$ mode (inset Fig. 2). We take advantage, as mentioned above, of the fact that the PMN modes do not change with x. Thus we fixed the two PMN modes and tracked the $E(1TO)$ mode. The results presented in Fig. 3 show that the soft mode frequency is constant for $0.2 \leqslant x \leqslant 0.8$ and then abruptly decreases for $x=0.1$. We assign stress to these frequencies by referring to Sanjuro *et al.*[19] and Cerdeira *et al.*[20] who showed that the soft-mode frequency decreases linearly with increasing pressure up to 12 GPa. The stress, plotted in Fig. 3, is estimated to be 2.5 GPa for $x=0.2-0.8$ (corresponding to PT layers of 26–104-Å thick). However, for $x=0.1$ (13-Å-thick PT layers) the stress increases to 3.6 GPa. This abrupt change can be the result of partial stress relaxation at a critical layer thickness l_c above which it is energetically more favorable for misfit dislocations to relax the strain in the SL. This effect has been observed in $PT_{0.5}/BT_{0.5}$ SL (Ref. 17), where l_c was observed to be >120 Å. Given the larger mismatch of the PMN/PT system and the asymmetric SL construction it is not surprising that the PMN/PT l_c occurs at this lower value.

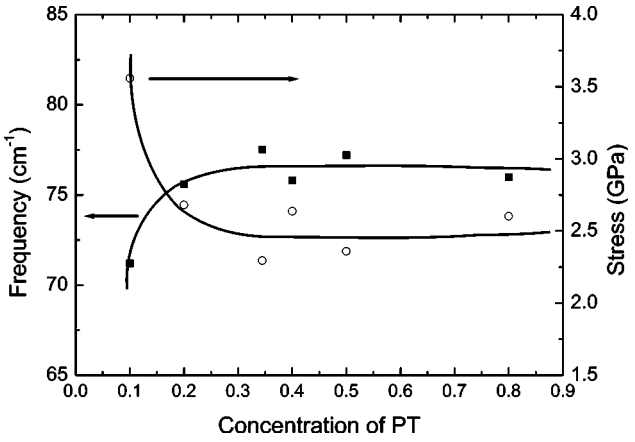

FIG. 3. Evolution of the frequency of soft mode $E(1TO)$ (■) and stress (○) as a function of x for $PMN_{(1-x)\Lambda}/PT_{x\Lambda}$ SL's.

Finally we present a result which also reflects the effect of stress on the PT modes. From the *VV* spectra of Fig. 2 for

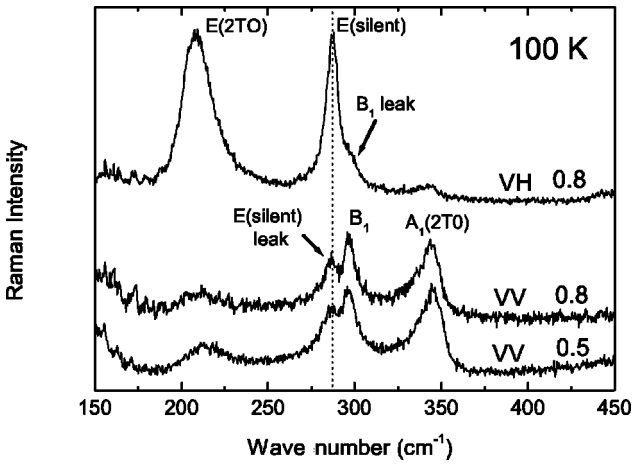

FIG. 4. Polarized Raman spectra *VV* and *VH* for SL $x=0.8$ and *VV* for SL $x=0.5$ measured at 100 K.

$x>0.3$, the band near 290 cm^{-1} can be decomposed into two peaks located at ~284 and ~293 cm^{-1}. We also took the *VV* spectra at 100 K so as to better resolve the peaks. In Fig. 4, we note the appearance of a new peak at 296 cm^{-1} and a weak mode located at 287 cm^{-1}. In PT, the T_{2u} silent mode of paraelectric O_h symmetry should be split into B_1+E modes in ferroelectric C_{4v} symmetry. The B_1 mode is Raman active and appears in *VV*. Such splitting has *not* been observed in PT crystals and the B_1+E peak located at 289 cm^{-1} is called a silent mode.[27,28] For $x=0.5$ and 0.8, the splitting of the silent mode is evident. The new mode at 296 cm^{-1} corresponds to the B_1 mode and the peak at 287 cm^{-1} corresponds to the leaked *E* silent mode that appears at the same frequency in the *VH* seen in Fig. 2 for $x=0.8$. This leakage phenomena, observed also for B_1 and $A_1(2TO)$ in *VH* geometry, into forbidden configurations has been attributed to the presence of domain walls in PT films. The 5-cm^{-1}-B_1-*E* mode splitting reported in Ref. 23 corresponds to an estimated stress of 2.1 GPa while in the $x=0.5$ and 0.8 SL's the mode splitting of 9 cm^{-1} corresponds to 2.6 GPa. Thus there is a correlation between the size of the B_1-*E* mode splitting and the magnitude of the stress in PT films and in our PT SL layers.

To conclude, we grew a series of $PMN_{(1-x)\Lambda}/PT_{x\Lambda}$ SL's for which the strains resulting from the lattice mismatch between the constituents is responsible for the *a*-axis orientation of the PT layers and produces both a frequency decrease of the PT vibrational modes and a splitting of the "silent mode" that does not take place in single crystal PT. We observe no indications of stress dependence of the Raman spectra in the PMN layers in contrast with pressure studies on PMN single crystals.

This work was supported by the Region of Picardy and the Regional European Development Funds.

*Electronic address: mimoun.elmarssi@u-picardie.fr

[1] S. W. Choi, T. R. Shrout, S. J. Jang, and A. S. Bhalla, Ferroelectrics **100**, 29 (1989).
[2] S. E. Park and T. R. Shrout, J. Appl. Phys. **82**, 1804 (1997).
[3] G. Burns and F. H. Dacol, Phys. Rev. B **28**, 2527 (1983).
[4] G. A. Samara, Solid State Phys. **56**, 239 (2001).
[5] C. Tantigate, J. Lee, and A. Safari, Appl. Phys. Lett. **66**, 1611 (1995).
[6] G. R. Bai, S. K. Streiffer, P. K. Baumann, O. Auciello, K. Ghosh, A. Munkholm, C. Thompson, R. A. Rao, and C. B. Eom, Appl. Phys. Lett. **76**, 3106 (2000).
[7] Z. Kighelman, D. Damjanovic, and N. Setter, J. Appl. Phys. **89**, 1393 (2001).
[8] G. Catalan, M. H. Corbett, R. M. Bowman, and J. M. Gregg, J. Appl. Phys. **91**, 2295 (2002).
[9] M. Tyunina, J. Levoska, K. Kundzinsh, and V. Zauls, Phys. Rev. B **69**, 224101 (2004).
[10] N. Lemée, H. Bouyanfif, F. Le Marrec, M. G. Karkut, B. Dkhil, J. Chevreul, and J. M. Kiat, Ferroelectrics **288**, 277 (2003).
[11] V. G. Koukhar, N. A. Pertsev, and R. Waser, Phys. Rev. B **64**, 214103 (2001).
[12] S. P. Alpay and A. L. Roytburd, J. Appl. Phys. **83**, 4714 (1998).
[13] J. S. Speck and W. Pompe, J. Appl. Phys. **76**, 466 (1994).
[14] Z. Li, C. M. Foster, D. Guo, H. Zhang, G. R. Bai, P. M. Baldo, and L. E. Rehn, Appl. Phys. Lett. **65**, 1106 (1994).
[15] K. S. Lee and S. Baik, J. Appl. Phys. **87**, 8035 (2000).
[16] Y. K. Kim, K. Lee, and S. Baik, J. Appl. Phys. **95**, 236 (2004).
[17] F. Le Marrec, R. Farhi, M. El Marssi, J. L. Dellis, M. G. Karkut, and D. Ariosa, Phys. Rev. B **61**, R6447 (2000).
[18] J. C. Jiang, X. Q. Pan, W. Tian, C. D. Theis, and D. G. Schlom, Appl. Phys. Lett. **74**, 2851 (1999).
[19] J. A. Sanjurjo, E. Lopez-Cruz, and G. Burns, Phys. Rev. B **28**, 7260 (1983).
[20] F. Cerdeira, W. B. Holzapfel, and D. Bäuerle, Phys. Rev. B **11**, 1188 (1975).
[21] D. Valim, A. G. S. Filho, P. T. C. Freire, J. M. Filho, C. A. Guarany, R. N. Reis, and E. B. Araujo, J. Phys. D **37**, 744 (2004).
[22] W. Ma, M. Zhang, T. Yu, Y. Chen, and N. Ming, Appl. Phys. A: Mater. Sci. Process. **66**, 345 (1998).
[23] S. Lee, H. M. Jang, S. M. Cho, and G. C. Yi, Appl. Phys. Lett. **80**, 3165 (2002).
[24] O. Svitelskiy, J. Toulouse, G. Yong, and Z. G. Ye, Phys. Rev. B **68**, 104107 (2003).
[25] M. El Marssi, R. Farhi, and Yu. I. Yuzyuk, J. Phys.: Condens. Matter **10**, 9161 (1998).
[26] J. Kreisel, B. Dkhil, P. Bouvier, and J. M Kiat, Phys. Rev. B **65**, 172101 (2002).
[27] C. M. Foster, Z. Li, M. Grimsditch, S. K. Chan, and D. J. Lam, Phys. Rev. B **48**, 10 160 (1993).
[28] G. Burns and B. Scott, Phys. Rev. B **7**, 3088 (1973).